Review article

In situ investigation of chemical processes by X-ray diffraction technique.
Studies of metal hydrides formed during electrochemical evolution of hydrogen

Remigijus Juškėnas*

Department of Materials Structure, Institute of Chemistry, A. Goštauto 9, LT-01108 Vilnius, Lithuania

Studies of nickel hydride formation during electrochemical hydrogen evolution on the nickel cathode are reviewed. Particular attention has been given to the use of X-ray diffraction (XRD) method *in situ* as well as *ex situ*. The formation of the nickel hydride in acid and alkaline media with promoters such as thiourea, As_2O_3, Sb and GeO_2 is considered.

Key words: X-ray diffraction, metal hydrides

INTRODUCTION

X-ray diffraction (XRD) has been used in chemical science and industry for nearly as long as a hundred years. As the beginning of this wide use can be considered the year 1916 when the so-called powder method was found by Debye and Scherrer. Up to this date, studies of X-ray diffraction were performed only with monocrystals. The discovery of the powder method, also called the polycrystal method, expanded the use of XRD both in science and industry. XRD methods were constantly improved and this opened new possibilities of their application. One of them is the use of XRD technique in *in situ* studies of chemical and electrochemical processes. As an example of a successful use of this method, studies of metal hydrides can be presented. They reflect the wide possibilities of XRD technique, such as determination of phase composition, evaluation of internal structure of crystallites (their size and microdeformations), measurement of stresses. All the above characteristics can be evaluated by XRD technique in the course of hydrides formation, this circumstance being of vital importance due to the fact that hydrides of many metals (*e.g.*, Ni) are unstable and rapidly decompose with a decrease in hydrogen pressure.

* E-mail: juskenas@ktl.mii.lt

Investigation of formation of metal hydrides and possibilities of their use in the recent decades have become important both for electrochemistry and studies of materials. Metal hydrides are associated, directly or indirectly, with electrodes used in new current sources, fuel cells and electrolysers. Knowledge of the regularities of hydrogen absorption and hydrides formation is essential for corrosion control when seeking to protect metals from the phenomenon of hydrogen brittleness. Penetration of hydrogen into metals hinders its use of it as a fuel in aircraft and spaceship technologies. Most of the recent works dealing with hydrides are devoted to hydrides formation in nickel-based metal alloys. However, there remain actual and not yet solved problems associated with peculiarities of nickel hydride formation in nickel electrodes charged with hydrogen in both acid and alkaline solutions. It is not clear why the amount of nickel hydride formed in alkaline solutions is lower than that formed in acid solutions under the same charging current density and what is the mechanism of promoter accelerating action during hydride formation.

1. The very first studies of nickel hydride by XRD technique

It has long since been known that nickel hydride is formed during cathodic hydrogen evolution on nickel electrode [1–3] or when nickel is saturated with

hydrogen in the hydrogen gas atmosphere of high pressure [4]. As early as the beginning of 1960 the regularities of nickel hydride formation were started to be studied by using both the electrochemical methods [2, 3] and XRD technique [5–8]. Two of the nickel hydride phases have been determined to form: α-NiH$_x$ and β-NiH$_x$ with $x \leq 0.03$ for the first phase and $x \approx 0.7$ for the second phase. It has been proved [3] that the α-NiH$_x$ phase always forms first, whereas the formation of β-NiH$_x$ requires more time, a sufficiently high density of the charging current i_H and a temperature not higher than 80 °C. Besides, this phase is formed at a greater speed and is more abundant in the presence of promoters such as thiourea, As$_2$O$_3$ and H$_2$SeO$_3$ [2]. From measurements of the volume of hydrogen absorbed in nickel it has been calculated that the H/Ni ratio in cathodically charged Ni electrodes varies from 0.1 to 0.9, depending on the cathode potential E_c and the temperature of the solution [3].

Both phases of Ni hydride are unstable and, after interruption of the charging current, they become decomposed within several hours (those formed without promoters within 3–5 min) [7]. It has been established by XRD technique that the crystal lattice of the β-NiH$_x$ phase is cubic, face-centered, similar to that of nickel, with the difference that its constant a is about 6% higher [7]. Later on the exact values of the lattice parameter a for the β-NiH$_{0.7}$ and β-NiD$_{0.7}$ phases have been determined: 0.37251 ± 0.00008 and 0.37191 ± 0.0008 nm, respectively [8]. The use of the neutron diffraction method made it possible to establish that in the course of formation of the NiH β phase the hydrogen atoms occupy octahedral, but not tetrahedral cavities in the face-centered cubic crystal lattice of nickel [9]. By the XRD method the kinetics of nickel hydride decomposition has been studied. [6, 10–13]. There is no general agreement among authors regarding the kinetics of β-NiH$_{0.7}$ phase decomposition: some of them state that it is a first-order kinetics [6, 10] whereas the others negate this [13]. For the deformed nickel foils the decomposition rate constant of the hydride phase has been found to be higher [12]. Diffusion of hydrogen is considered to occur through both the boundaries of crystallites and twins, dislocations and the crystal lattice [13].

Monev and others [14] who studied a change in internal stresses of nickel coatings during cathodic charging and after its interruption noticed a change in a hydride lattice parameter. They determined by the XRD *ex situ* method that 4–16 minutes after interruption of charging $a = 0.3756$–0.3747 nm, and after 56–76 minutes the value decreased up to 0.3734–0.3711 nm. Such change in the parameter of the hydride phase lattice was attributed by the authors to the formation of solid solution of hydrogen in hydride phase during the process of charging.

2. Early XRD *in situ* investigations of nickel hydride

Though it is obvious that for investigation of such unstable phases as nickel hydride the *in situ* methods could be very useful, publications dealing with nickel hydride studies by XRD *in situ* are rare. Polukarov with co-workers [15] investigated a change in the parameters of the fine internal structure of Ni crystallites *versus* the number of charging-discharging cycles in H$_2$SO$_4$ solution with thiourea. As soon as after one cycle the size of X-ray coherent scattering blocks D was found to decrease by 1.5–2 orders. Little attention was paid in this work to regularities of nickel hydride formation or decomposition. The β-NiH$_x$ phase was determined to form at $i_H \geq 5$ mA cm^{-2}, but to hold the formed amount of hydride phase in the cathode, $i_H \approx 2$ mA cm^{-2} is sufficient. At the beginning of the charging process an increase in the parameter of nickel crystal lattice was found to be as low as 3%, a higher increase (by 6%) in the a value having been obtained only at the end of the process, *i.e.* when almost all the nickel foil was turned into nickel hydride.

3. The problem of bulk nickel hydride formation in alkaline media

All the above studies were performed during the cathodical charging of nickel in acid medium or during its saturation in hydrogen gas. From the practical point of view, it is much more important to study the regularities of nickel hydride phase formation in alkaline media, as it is alkaline solutions that are used in the electrolysers designed for hydrogen production and also in the current sources. XRD investigations of nickel hydride formation in alkaline solution are described only in [16]. By watching the nickel cathode potential in the promoter-free alkaline solution at a hydrogen current density 300 mA cm^{-2}, the E_c was found to become more negative by ~500 mV within an hour. Under such conditions the nickel cathode was charged with hydrogen for 2 h and then, following 20 min after switching the polarisation off, its diffractogram was recorded with two weak but clear peaks of β-NiH$_x$. After adding 1 g dm^{-3} As$_2$O$_3$ into the solution, the Ni cathode potential at a current density 300 mA cm^{-2} immediately (within several minutes) became more negative by ~350 mV and, as is seen from the intensity of XRD peaks, a much larger amount of hydride phase was formed. Based on these data, the authors state that it is the nickel hydride that accounts for an increase in the hydrogen evolution overvoltage η_H.

In the literature there are no data nickel hydride formation in alkaline medium by using the XRD *in situ* technique. Baranowski in his early works [3] doubted the possibility of nickel hydride β-phase formation during the charging of nickel in alkaline solutions, and later on [17] he expressed a belief that

in alkaline solutions the bulk β-NiH$_x$ is not formed. According to him, in alkaline solutions only the surface nickel hydride or semi-surface one can be formed, whereas the bulk nickel hydride, which in acid medium can be obtained in desirable amounts [18] and which can be fixed by XRD technique is not formed. We also failed to find works dealing with the question why at the same charging current density the formation of nickel hydride in acid medium is much easier and more abundant than in alkaline medium. It is not improbable that this is related to a different mechanism of hydrogen evolution reaction (HER) in acid and alkaline solutions.

When summarising the literature on nickel hydride, one can see a lack of XRD *in situ* studies dealing with regularities of nickel hydride formation, especially in solutions without promoters and in alkaline solutions where formation of hydride phase is less abundant. Not much data are also available about the influence of promoters on hydride formation. To fill this gap, in our laboratory we performed studies of nickel hydride formed during hydrogen evolution on a nickel cathode by using the XRD *in situ* and *ex situ* techniques [19–22]. By using a cell designed at the laboratory for XRD *in situ* studies of electrochemical processes, the formation of CuH during chemical deposition of copper was also studied [23].

4. Electrolytic cells for XRD *in situ* studies

More than 40 years ago, first attempts were made to use the XRD *in situ* method for investigation of phase changes occurring in the electrodes (including their surface layer) of alkaline cadmium-nickel accumulators during the process of their charging-discharging [24, 25]. Besides, attempts were made to study changes occurring in the internal structure of metal coatings during the process of their electrocrystallisation [26–28]. In 1990–91, at the Institute of Chemistry some electrolytic cells for XRD *in situ* studies were designed and tested [19].

The cells described in the literature can be divided into 3 groups:

• Cells in which part of the electrode being studied by the XRD method emerges periodically from the electrolyte solution [26–28];

• Cells in which during XRD studies the electrode is pressed to the window made in one of the cell walls by using an X-ray transparent material [29–31];

• Cells in which the electrode being investigated by XRD method serves at the same time as one of the cell walls [15].

Each of these cells has its advantages and shortages. In cells of the first type the electrode under study is not exactly in the same conditions of electrolysis as during a traditional electrochemical experiment, because part of the electrode periodically emerges from the solution and has a contact with air. In the second type cells, in order to reduce X-ray absorption and dispersion in the solution, the electrode studied is pressed as close as possible to the wall surface and so the conditions of electrolysis are again disturbed, as diffusion limitations are in this case unavoidable. As regards the exactness of an electrochemical experiment, most acceptable seems to be the third type cell, but in this case arise some problems, sometimes insurmountable, associated with production of the electrode studied. The electrode needs to be transparent to X-ray, *i.e.* rather thin, so that the X-rays after diffraction in crystallites present on the electrode surface, which is in contact with the solution, remained sufficiently intensive. As such an electrode can serve a nickel foil maximum 8–12 µm thick. However, making such a foil is impossible when the metal or alloy coating is characterized by great internal stresses.

6. Tests of the cell for XRD *in situ* studies

As the third type cell is the simplest one from the technical point of view, it was the first one that was produced ant tested at our laboratory. Its scheme is shown in the drawing (Fig. 1). To clear up the possibilities of its use, formation of electrolytic copper coating in sulphate electrolyte was studied (in these coatings Cu$_2$O was found by some investigators by means of electronography). A discussion was started on the question at what stage the oxide becomes formed: during electrocrystalisation process or after removing the coating from the solution. In the XRD *in situ* studies, as a cathode was used ~50 nm thick Cu film evaporated in vacuum on an 8 µm thick PETF film. The recorded XRD patterns showed an increase in Cu coating thickness during electrolysis, but Cu$_2$O peaks were not fixed. This is not a proof that during the process Cu(I) oxide is not formed at all, but only a proof that it is not formed in significant amounts detectable by XRD.
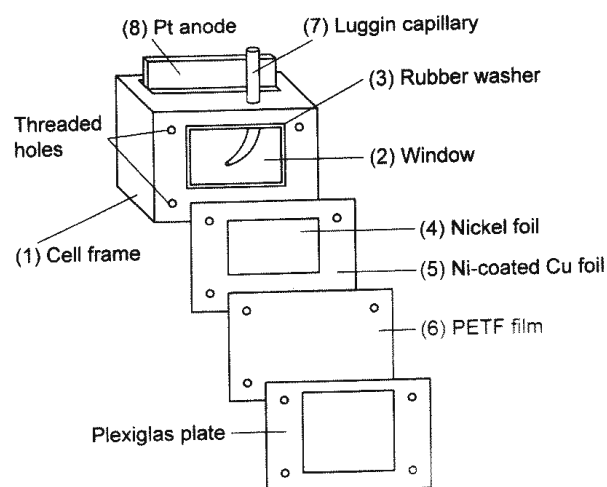

Fig. 1. Schematic representation of the electrolytic cell for *in situ* XRD investigations

Another study performed during the cell tests was devoted to evaluation of interdiffusion between electrolytic coating and cathode metal atoms in the process of electrocrystallisation. The used PETF film was prepared similarly as in the first case, the only difference being that on the Cu film, evaporated in vacuum, a 5 μm thick Cu coating was electroplated additionally. On this Cu electrode, electrodeposition of Zn from zincate electrolyte in the cell for XRD *in situ* studies was performed with a simultaneous recording of the diffractogram. At a cathodic polarisation of 100 mV, as soon as 20 min after the beginning of electrodeposition, the ε-CuZn$_3$ intermetallic phase was detected. This was a proof of a rather quick metal interdiffusion due to which the intermetallic phase is formed not only on a thin surface coating/cathod layer (this has been already determined by the method of cyclic voltammetry), but also in a larger volume of a micron order. Later the regularities of Cu and Zn interdiffusion were studied in more detail by using the XRD *ex situ* technique [32].

The third experiment performed with this cell dealt with NiH formation during cathodic evolution of hydrogen on a nickel electrode in 1N H$_2$SO$_4$ solution with 0.2 g dm^{-3} thiourea and without it. The electrode for the study was produced in another way than in the first two cases, the reason for this being high internal stresses of nickel electrolytic coatings (they used to peel off from the PETF film soon) deposited even from sulphamate solution. For producing a 8–10 μm thick nickel foil, a Ni coating of this thickness was deposited on a 50 μm thick copper foil (Fig. 1 (5)) and then, by using 50 g dm^{-3} H$_2$SO$_4$ and 500 g dm^{-3} CrO$_3$ aqueous solution, there was etched in copper a 15 × 15 mm "window" for X-rays (Fig. 1 (4)). Such a nickel coating foil with a frame of copper was attached to the cell wall in which a window of a corresponding size was cut out (Fig. 1 (2)). On the external side of the nickel foil the PETF film was put on to prevent the electrolyte outflow from the cell in case of cracks occurrence in the foil. The nickel foil and the PETF were pressed up to the cell body by using a frame made of a 4 mm thick plexiglass plate and four bolts. Such nickel electrode was used for studies of NiH formation kinetics during cathodic charging as well as hydride decomposition kinetics after switching off the polarisation. It was found *for the first time* that during the process of charging not only the intensity of hydride phase XRD peaks but also the position of their maximum, *i.e.* an X-ray diffraction angle $2\theta_{max}$ that corresponds to the maximum of intensity are changed. Once this angle is determined, the crystal lattice parameter *a* can be calculated. It has been found that during the charging process the *a* va-

lue increases from 0.3725 nm to 0.3741 nm (for nickel *a* = 0.3524) and after interruption of polarisation the *a* value decreases to 0.3727 nm within ~5 min. A change in the hydride NiH$_x$ stoichiometric coefficient *x* has been assumed.
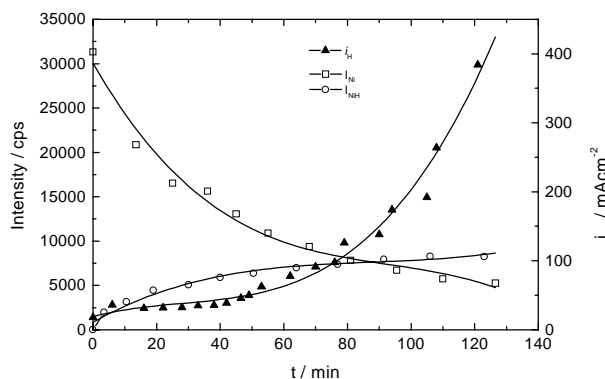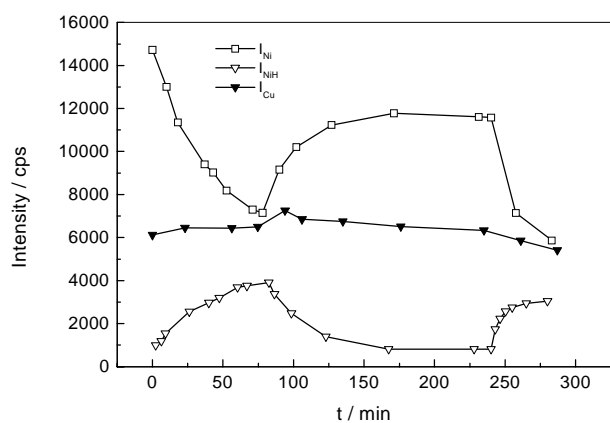

Fig. 2. Time variations of the intensity of diffraction lines β-NiH$_x$ (200) and Ni(200) and of charging current density i_H during charging in solution containing 0.2 g dm^{-3} of thiourea at E_c = −450 mV

6. Variation of stoichiometric coefficient *x* of the phase β-NiH$_x$

6.1. Variation of 2Θ angle of XRD peaks corresponding to the β-NiH$_{0.7}$ phase

Nickel hydride in work [19] was only one of the three chosen objects suitable for XRD *in situ* studies. However, after detecting the effect of a change in the position of NiH$_x$ XRD peak maximum, which had not been described in the literature earlier, we decided to study this effect in more detail [20].

The above described cell designed for XRD *in situ* studies was used. The nickel foil was electrodeposited from the Watts-type solution: NiSO$_4$ 7H$_2$O 240, NiCl$_2$ 6H$_2$O 45, H$_3$BO$_3$ 30 g dm^{-3}, pH 4.8, t = 50 ± 1 °C, i_d = 20 mA cm^{-2}. XRD studies of Ni foil showed that it was strongly textured in the direction <100>. Ni was charged in 1M H$_2$SO$_4$ solution with various amounts of thiourea (0÷5 g dm^{-3}). To establish as precisely as possible within the shortest time the angle of X-ray diffraction $2\theta_{max}$, a special method was used. For exact determination of the lattice parameter *a* of the hydride phase as a function of cathode potential or current density, both the phase amount and the lattice parameter must be kept constant during the measurement. When looking for such conditions, a change in the intensity of peaks β-NiH$_x$(200) and Ni(200) with time at a constant potential E_c was studied. Figure 2 shows typical data obtained for charging of Ni in the solution with 0.2 g dm^{-3} thiourea at a cathodic potential of −450 mV. Under these conditions the hydride quantity stopped changing after 100–120 minutes from the beginning of charging.

Fig. 3. Time variations of the intensity of diffraction lines Ni(200), Cu(200) and β-NiH$_x$ (200) during cathodic charging in solution containing 0.2 g dm^{-3} of thiourea at E_c = –350 mV (t = 0–78 min and t = 240–260 min) and when polarization was switched off (t = 78–240 min)
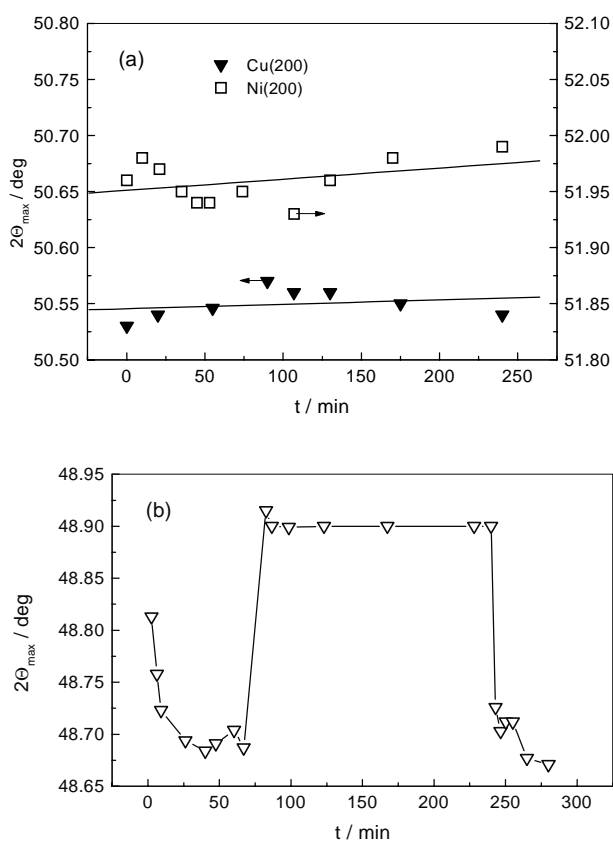

Fig.4. Time variations of $2\Theta_{max}$ of diffraction lines Ni(200), Cu(200) (*a*) and β-NiH$_x$ (200) (*b*) during cathodic charging in solution containing 0.2 g dm^{-3} of thiourea at E_c = –350 mV (t = 0–78 min and t = 240–260 min) and when polarization was switched off (t = 78–240 min)

After switching off the charging current the amount of hydride decreases and that of nickel phase increases (Fig. 3, t = 78 min). In about 160 min (240–78 ≈ 160 min) the β-NiH$_x$ phase becomes decomposed. When the charging is repeatedly started (Fig. 3, t = 240 min),

hydride is formed in a much shorter time. This is associated with changes in the internal structure of nickel occurring during the charging: atomic hydrogen occupies octahedral cavities of the nickel lattice and thus causes high internal stresses due to which the density of dislocations becomes much higher and the size of X-ray coherent scattering blocks becomes lower [15].

Figure 4 shows the variation of the position of maximums of Ni(200), Cu(200) and β-NiH$_x$ (200) XRD peaks $2\theta_{max}$ in the process of charging. The maximums of the first two peaks do not change within limits of errors, whereas the $2\theta_{max}$ angle corresponding to the maximum of the hydride peak diminishes. After switching off the charging current (t = 78 min), the angle of the maximum rapidly increases up to ~48.90°, and when the charging current is switched on repeatedly it decreases to ~48.68°. Such shift makes up 0.45% of the $2\theta_{max}$ value, with an error of the measurement as small as 0.025%. After calculation the hydride lattice parameter *a* from the average value of the minimum $2\theta_{max}$ angle, the value 0.37400 ± 0.00005 nm was obtained. The parameters of Ni and Cu lattices calculated from the simultaneously performed measurement data were 0.35202 ± 0.00003 and 0.36120 ± 0.00005 nm, respectively. The corresponding values of lattice parameters for these metals presented in reliable sources [33] are 0.35238 and 0.36150 nm, *i.e.* on average by 0.00033 nm higher than those obtained by us. After introducing this correction, the value of the lattice parameter of β-NiH$_x$ phase becomes equal to 0.37433 nm. When polarisation is switched off after the charging for 78 min, the hydride phase value diminishes within 5 min to 0.37280 nm.
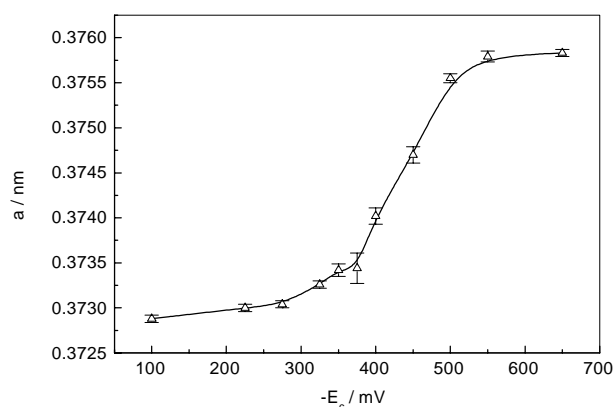
Fig. 5. Dependence of β-NiH$_x$ phase lattice parameter *a* on cathode potential E_c in solution containing 5 g dm^{-3} thiourea

A minimum value of $2\theta_{max}$ angle corresponding to the peak β-NiH$_x$ (200) maximum depends on the electrolysis conditions (cathodic current density or the potential and concentration of promoter in the solution). Figure 5 shows how the lattice parameter of the β-NiH$_x$ phase depends on the cathodic potential in 1 M H$_2$SO$_4$ solution containing 5 g dm^{-3} thiourea.

6.2. Possible reasons for diffraction angle variation

The possible reasons for the variation of $2\theta_{max}$ angle of the XRD peak can be: 1) deformation defects in cubic face-centered metals, which can lead to a slight shift of the peak, and crystal twins which can cause an asymmetry of the peak and a slight shift of the diffraction angle; 2) internal stresses of the coating, which can result in a shift of the peak maximum, this variation being proportional to the magnitude of stresses; 3) the composition of the solution, which can have an influence on the solid solution lattice parameter a and on $2\theta_{max}$.

It has been determined [15] that nickel hydride is formed from small (20–20 nm) coherent X-ray scattering blocks and is characterized by large microdeformations ($\Delta d/d = 2.8 \times 10^{-3}$) as well as numerous packing deffects ($\alpha = 0.01–0.014$). We calculated what a shift of the diffraction peak β-NiH$_x$ (200) $2\theta_{max}$ would yield due to packing defects at a concentration of $\alpha = 0.01–0.014$ and have obtained a value 0.036–0.05°, *i.e.* $\Delta 2\theta$ 4–5 times less as compared with that established by us.

Nickel coatings are characteristic of internal stresses, and besides they undergo changes during the charging process [14]. In the nickel coating obtained from the Watts-type electrolyte the magnitude of internal stresses reaches 30–50 N mm^{-2}. As is mentioned above, the magnitude of internal stresses of the coating can be determined from the diffraction peak shift:

$$\sigma \approx (E/\nu)\, ctg(\Theta_{max})\Delta\Theta_{max}, \qquad (1)$$

where σ is magnitude of internal stresses, E is Young's modulus (for nickel 205000 N mm^{-2}), ν is Poisson's coefficient (0.3–0.34), $\Delta\theta_{max}$ is the difference between θ_{max} for a sample with internal stresses and for a sample without stresses. If we assume that internal stresses in the charged nickel foil reach 50 N mm^{-2}, the peak shift caused by them would be 0.0043°. Hence, neither internal stresses can be the reason for the changes in $2\theta_{max}$ value observed by us.
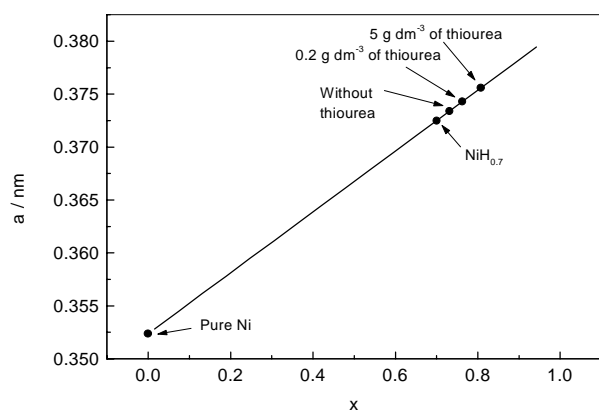
6.3 Variation of the stoichiometric coefficient of β phase

A comparison of the influence of all known factors on the $2\theta_{max}$ value allows to state that the variation of the β-NiH$_x$ (200) diffraction peak $2\theta_{max}$ value during charging and after its interruption is caused by changes in the stoichiometric coefficient x of this phase. In the opinion of other authors [14], this shift is related to the formation of a solid solution of hydrogen in the β-NiH$_{0.7}$ phase when, after switching off the charging current, hydrogen evolution from the hydride phase occurs. As our studies have shown, the diffraction peak of the hydride phase shifts towards the smaller angles in the process of charging, but just after its interruption $2\theta_{max}$ decreases. By the method of neutron diffrac-

tion it has been established that hydrogen atoms occupy octahedral cavities in the nickel crystal lattice. If they all were filled with H atoms, the ratio H / Ni would be equal to 1. In the opinion of some authors [2], the ratio H / Ni = 0.7, being characteristic of nickel hydride β phase, can be a result of filling up the holes of nickel d-shell by hydrogen electrons. When the H / Ni ratio exceeds 0.7 and the hydrogen absorbtion still persists, the absorbed hydrogen atoms can be treated as additional ones, in the sense that for them there are no free holes left in the d-shell any more, though in the nickel crystal lattice they occupy analogous (from the crystallographic point of view) positions, *i.e.* octahedral cavities. Therefore, they cannot be considered as those forming a solid solution in hydride β phase. However, the number of electrons common to nickel and hydrogen, which falls on average per one atom of hydrogen, starts to decrease and probably due to this the Ni–H bond becomes weaker. After switching off the charging current, the excess H atoms easily move away from the nickel hydride crystal lattice, this being a reason for a shift of the diffraction peak, but not for a change in the peak intensity. The β-NiH$_x$ phase itself could be treated as a solid solution, since hydrogen content can vary continuously. Vegard's law is valid for a solid solution, according to which the lattice parameter of the latter depends linearly on the content of dissolved atoms. In the case of the hydrogen solid solution in the nickel there are two well defined points of the above mentioned linear dependence: 1) pure Ni ($x = 0$; $a = 0.35238$) and 2) β-NiH$_{0.7}$ phase ($x = 0.7$; $a = 0.3725$ nm). Through these two points a line can be drawn (Fig. 6). After putting on it the maximum a values determined during charging Ni in the solutions with different thiourea amounts, we obtain the highest x or H / Ni values that can be reached under the given conditions. In 1 M H$_2$SO$_4$ solution without thiourea x can be increased to 0.73; in the solution with 0.2 g dm^{-3} thiourea the stoichiometry coefficient reaches 0.76; with 5 g dm^{-3} thiourea the x value rises up to 0.81.

If nickel hydride were a solid solution of hydrogen in all intervals of H / Ni or x values, the parameter of the hydride phase lattice would vary continuously from 0.35238 nm to ~0.380 nm. However, nobody had detected NiH$_x$ with the lattice parameter a smaller than 0.3725 nm, with *i.e.* the x value smaller than 0.65–0.7. In our opinion, β nickel hydride may be considered as the NiH$_x$ phase with the stoichiometric coefficient x equal to or larger than ~0.7.

The summary data obtained by us and other investigators allow to state that at the beginning of nickel cathodic charging the formation of α-NiH$_x$, where x ≤ 0.03, occurs; then, with continuing the evolution of hydrogen, formation of β phase starts;

Fig. 6. Dependence of calculated (solid line) and experimental (•) values of the lattice parameter a of β-NiH$_x$ phase on the stoichiometric coefficient x of the hydride phase

when this phase is formed but hydrogen evolution is still in progress, the empty octahedral cavities in the crystal lattice of β-NiH$_{0.7}$ phase start to be filled up, this being expressed by an increase in the lattice parameter a. After interruption of the charging, the excess atoms of hydrogen remove the first, this being the reason for a decrease in the a value to the value characteristic of β-NiH$_{0.7}$ phase; with proceeding the desorption of hydrogen, the amount of the latter phase diminishes and no changes in the a or x value are observed any more.

7. Formation of nickel hydride in alkaline solutions

7.1 XRD in situ *studies of nickel hydride formed in alkaline media*

In the next stage of our studies we dealt with formation of nickel hydride during cathodic evolution of hydrogen in alkaline solutions. Since in alkaline media thiourea does not act as a promoter of hydride formation process, we used As$_2$O$_3$, which is active in the whole range of pH values. By using the electrolyte cell designed for XRD *in situ* studies, nickel foil was charged in 3M KOH solution with 2 g dm^{-3} As$_2$O$_3$. After switching on a 300 mA cm^{-2} current, at the beginning the amount of β-NiH$_{0.7}$ phase increases, but after 4–5 min it starts to decrease (Fig. 7). After 10 minutes from the start of the charging, the β-NiH$_{0.7}$ phase becomes undetectable by XRD technique any more. An analogous behaviour of the hydride phase was fixed at higher densities of the hydrogen current, up to 800 mA cm^{-2} inclusive. The attained maximum amount of β-NiH$_{0.7}$ phase V_{NiH} (the volume fraction expressed in %) was not higher than 1%, whereas in acid media it was as high as 70%. Several reasons for the formation of low amounts of hydride phase are possible: 1) full consumption of all the promoter; 2) increase in the temperature of the solution due to a high current density; 3) differences in the mechanism of hydrogen evolution reaction (HER) in acid and alkaline media.
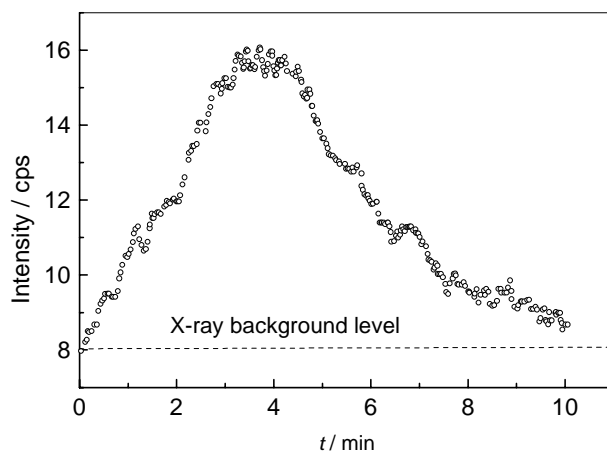

Fig. 7. Variations of intensity at the maximum of the XRD peak β-NiH$_x$ (200) as a function of the nickel cathode charging time in alkaline solution with 2 g dm^{-3} As$_2$O$_3$ at a constant current density of 300 mA cm^{-2}

7.2 Search for the reasons responsible for small amounts of nickel hydride formed in alkaline solutions

7.2.1 Studies of promoter exhaustion

To verify the first reason, we investigated the dependence of V_{NiH} on the electric charge Q passed through the alkaline solution used for charging. Several copper electrodes, covered with a 10–12 μm thick nickel coating deposited from the Watts' type electrolyte solution, were consecutively charged for 30 min each in the same 3M KOH solution containing 2 g dm^{-3} As$_2$O$_3$ by using a 150 mA cm^{-2} current density. Following no more than 2–3 min after the charging, Ni(200) and β-NiH$_x$ (200) XRD peaks were scanned and the value of V_{NiH} was calculated. The dependence obtained is shown in Fig. 8. It should be noted that the amount of the β-NiH$_x$ phase reached ~35%. After passing 1600–1700 C through the solution and subsequent charging of the Ni electrode in it, hydride was not detectable by XRD any more. Let us note this amount of charge as Q_0. By the method of X-ray fluorescence spectroscopy we determined the amount of As deposited on the surface of the electrodes under study. It was found to decrease rapidly with increasing the quantity of the charge passed through the solution (Fig. 8). As soon as hydride is not found in the charged electrode any more, arsenic is not found any more, either. So, the β-NiH$_x$ phase ceases to be detected when all the promoter is used up completely.

After increasing the As$_2$O$_3$ amount twice, Q_0 does not change noticeably (Fig. 8). But after increasing the volume of the solution used for charging from 25 to 50 ml, Q_0 becomes almost two times larger (Fig. 9). This could be related to diffusion limitations of AsO$_2^-$ particles. Besides, such relationship between Q_0 and the solution volume ex-
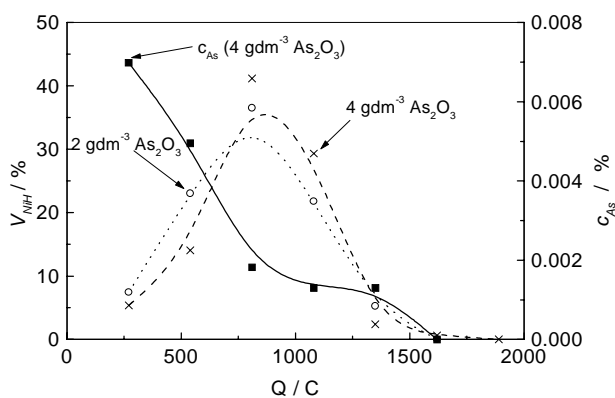
Fig. 8. Fraction by volume of β-NiH$_x$ phase formed in the Ni electrode in alkaline solution containing 2 and 4 g dm^{-3} of As$_2$O$_3$ at a constant current density of 150 mA cm^{-2} for 30 min as a function of the charge passed through the solution. Dependence of the surface content of As, c_{As}, on the charge passed through the solution

plains, at least partly, why in the cell designed by us for XRD *in situ* studies the hydride phase is observed only for a short time (5 min). One of the reasons for such a short-term existence of β-NiH$_x$ can be a small working volume (only 10 ml) of the cell.
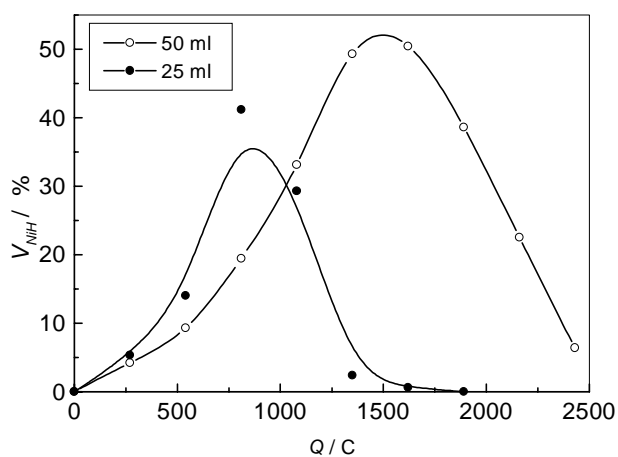
Fig. 9. Fraction by volume of β-NiH$_x$ phase formed in the Ni electrode at a constant current density of 150 mA cm^{-2} for 30 min as a function of the charge passed through the solution with 4 g dm^{-3} of As$_2$O$_3$

Our studies proved that during the charging of nickel in alkaline solution with AsO$_2^-$ particles the bulk β-NiH$_x$ (about 35 volume %) but not the surface or semi-surface one as reported by Baranowski [17] is formed. Both the hydride amount and its stability were sufficient for investigating this phase by the XRD *ex situ* technique. On the other hand, low amounts of hydride detected by the XRD *in situ* technique can be explained not only by a small volume of the cell, but also by different, as compared with a usual electrolytic cell, conditions of hydrogen absorption-desorption. In the cell designed for XRD *in situ* studies, a nickel foil which at the same

time serves as one of the cell walls is charged. So the portion of atomic hydrogen diffuses through the foil to its external surface and becomes desorbed here. Therefore, the amount of hydrogen sufficient for the formation of the bulk β-NiH$_x$ cannot be accumulated in the foil volume. During the first minutes after switching the charging current on the hydride does start to be formed, but it causes internal stresses and cracks in the foil as well as an increase in the density of dislocations. This facilitates hydrogen diffusion and thereby a decrease of its concentration in the foil as well as decomposition of the formed hydride.

7.2.2 Hydrogen desorption

In an ordinary electrolytical cell a Ni coating was charged on the copper base, which does not allow hydrogen to move away from nickel. It is known [34] that a unit of copper volume accumulates 0.6–4.8 volumes of hydrogen and nickel 18.0. To check up whether desorption of hydrogen affects the formation of hydride, in XRD *in situ* cell we used a nickel foil with the external side covered with a thin (0.5 μm) layer of copper transparent to X-rays. In the nickel foil prepared in such a manner the β-NiH$_x$ phase was detected by the XRD technique only as long as the charging current was flowing. It had to be $i_H \geq 150$ mA cm^{-2}. However, even for the current density 800 mA cm^{-2} the amount of the formed hydride V_{NiH} was found not to exceed 5%. This can be due to an incontinuous layer of copper on the external side of the foil or its insufficient thickness, these being the reasons for not a full stop of hydrogen desorption.
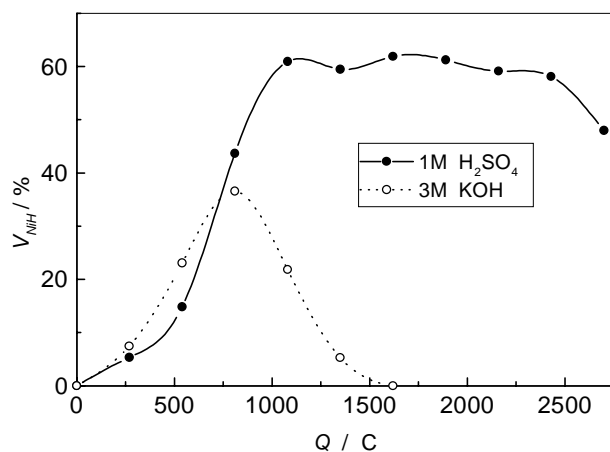
7.2.3 Influence of solution temperature
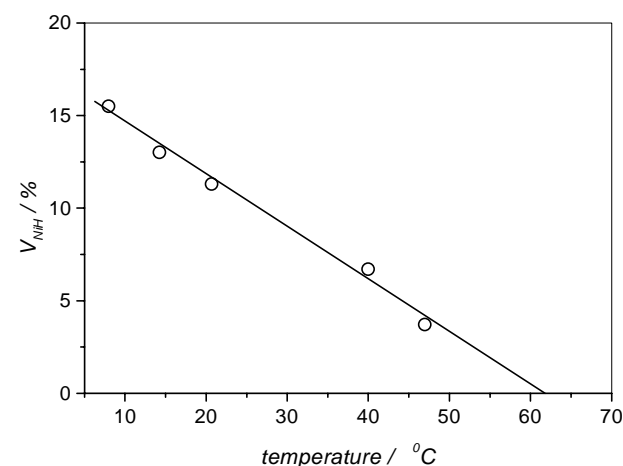
Fig. 10. Fraction by volume of β-NiH$_x$ phase formed in the Ni electrode at a constant current density of 100 mA cm^{-2} for 30 min as a function of the temperature of alkaline solution containing 2 g dm^{-3} of As$_2$O$_3$

As already mentioned, a reason for a low amount of hydride can also be an increase in the solution temperature caused by a high current density. The

influence of the solution temperature on formation of hydride was investigated in an ordinary cell by charging the Ni coating on Cu base under a current density of 100 mA cm^{-2} for 30 min. The obtained results are presented in Fig. 10. The amount of the hydride formed decreases linearly with increasing the temperature of the solution. When extrapolated, this dependence shows that the β-NiH$_x$ phase should not be detected any more upon reaching $t \approx +$ 60 °C in the solution. When in the cell designed for XRD *in situ* studies a current of 300 mA was passed for 15 min, the solution was found to warm up to ~ + 40 °C. Hence, heating of the solution can have an appreciable influence on hydride formation.

With the aim to compare more exactly the formation of β-NiH$_x$ phase in acid and alkaline media, we have established a relationship between V_{NiH} and the charge passed through the solutions containing the same promoter (As$_2$O$_3$). Each sample was charged with a current of 150 mA cm^{-2} for 30 min. In alkaline solution the promoter was found to be used up completely in a much shorter time than in acid solution (Fig. 11), possibly because of differences in the mechanism not only of HER, but also of the promoter. In acid medium the As^{3+} (at pH < 1, AsO$^+$) cations whereas in alkaline medium the AsO$_2^-$ anions take part in cathodic reaction.

formed hydride as a function of the charge passed or a serial number of the sample were measured for the solutions containing different quantities of As$_2$O$_3$. The obtained differences among the V_{NiH} values were especially clear in the first samples (Fig. 12). Figure 13 shows how arsenic oxide concentration affects the V_{NiH} value of the first sample charged in the solution. The maximum amount of β-NiH$_x$ phase was found to be formed in 3M KOH solution containing ~0.2 g dm^{-3} As$_2$O$_3$ This is an optimum amount of As$_2$O$_3$ in 3M KOH solution when we want to obtain as much nickel hydride as possible.

Fig. 12. Fraction by volume of β-NiH$_x$ phase charged with hydrogen one by one for 30 min in the same alkaline solution with different quantity of As$_2$O$_3$ at a constant current density of 150 mA cm^{-2} as a function of the sample serial number
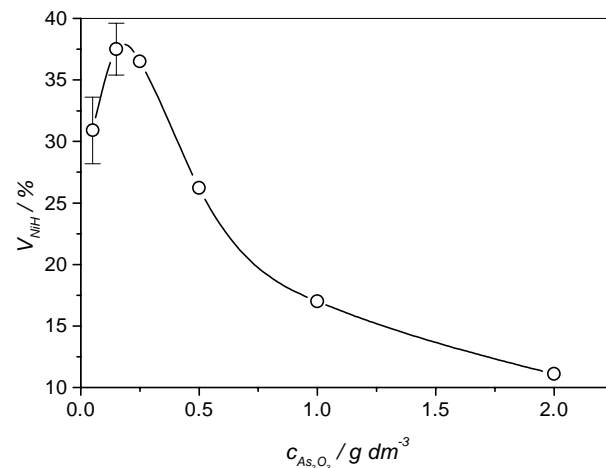
Fig. 13. Fraction by volume of β-NiH$_x$ phase formed in Ni electrode at a constant current density of 150 mA cm^{-2} for 30 min as a function of As$_2$O$_3$ quantity in 3 M KOH solution
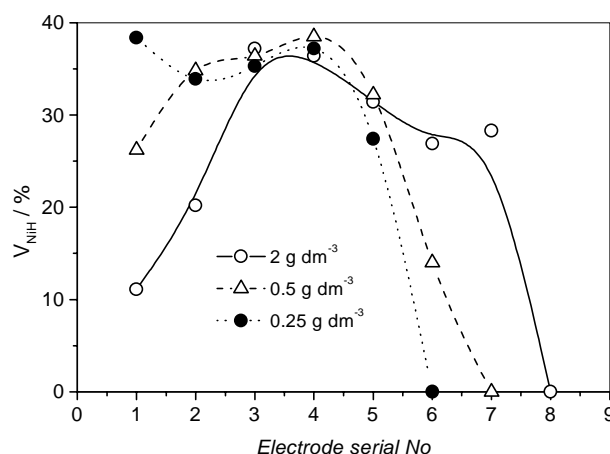

Fig. 11. Fraction by volume of β-NiH$_x$ phase formed in the Ni cathode during hydrogen evolution at a constant current density of 150 mA cm^{-2} for 30 min as a function of the charge passed through acid and alkaline solutions with 2 g dm^{-3} of As$_2$O$_3$.

7.2.4 Optimal conditions for nickel hydride formation in alkaline media

The V_{NiH} dependence on the charge passed through the solutions (Figs. 8–10) show that small amounts of hydride are formed not only where the promoter is used up completely, but also for the first samples where the amounts of the charge passed through the solution are not yet large. The amounts of the

Employing the optimum amount of the promoter we have determined a relationship between the V_{NiH} and the charging current density (every sample was charged for 30 min). The amount of hydride was found to increase with increasing the current density up to 100 mA cm^{-2} (Fig. 14). With a further

increase of i_H, the amount of the formed β-NiH$_x$ phase was found to become constant.

The relationship between V_{NiH} and the duration of charging indicates that the larger the current density the sooner V_{NiH} reaches the maximum value and starts to decrease (Fig. 15).
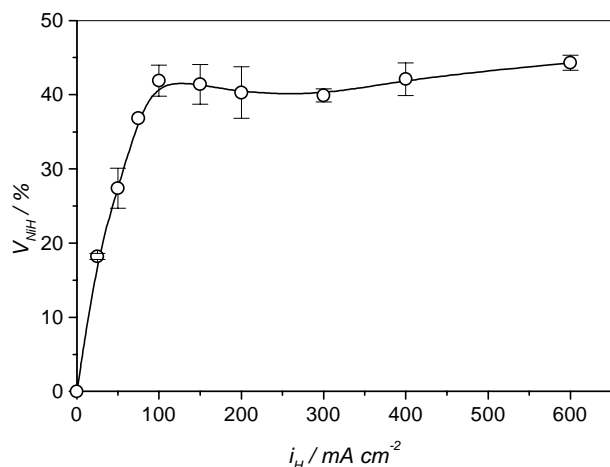
Fig. 14. Fraction by volume of β-NiH$_x$ phase formed in Ni electrodes charged with hydrogen for 30 min in 3 M KOH solution with 0.2 g dm^{-3} of As$_2$O$_3$ as a function of the hydrogen current density i_c
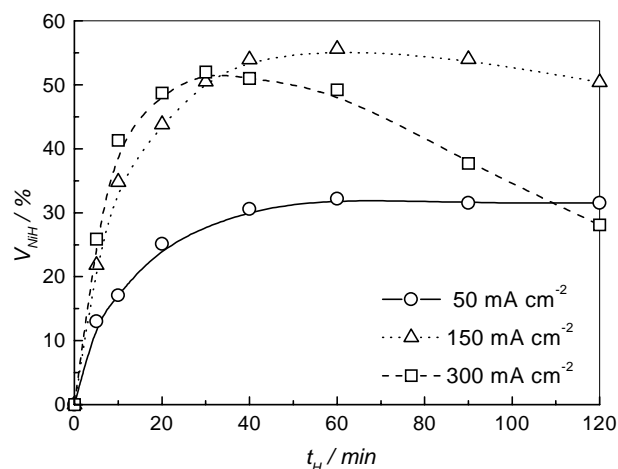
Fig. 15. Fraction by volume of β-NiH$_x$ phase formed in Ni electrodes charged with hydrogen under current density of 150 mA cm^{-2} in 3 M KOH solution containing 0.2 g dm^{-3} of As$_2$O$_3$, as a function of the charging time t_c

Table 1 shows how the concentration of alkali and the type of cation affect the amount of the hydride formed in the charging process. Ni coatings were charged for 30 min by a 150 mA cm^{-2} current in alkaline solutions containing 0.2 g dm^{-3} As$_2$O$_3$. Formation of nickel hydride was studied in KOH solutions of four concentrations, but no influence of the concentration was detected. In NaOH and NH$_4$OH solutions a slightly lower amount of hydride was formed, and in 0.5 M LiOH solution the least V_{NiH} value was obtained.

Table 1. **Dependence of the β-NiH$_x$ phase volume fraction on alkali and its concentration, c in solution containing 0.2 g dm^{-3} of As$_2$O$_3$. Charging current density i_c = 150 mA cm^{-2}, charging time t_H = 30 min**

c (mol dm^{-3})	V_{NiH} (%)			
	KOH	NaOH	NH$_4$OH	LiOH
0.5	50.8 ± 2.8			39.5 ± 1.7
1.0	51.8 ± 1.2			51.9 ± 1.3
3.0	51.4 ± 2.7	48.9 ± 1.8	46.8 ± 2.1	52.9 ± 2.4
6.0	50.9 ± 1.8			

7.3 Other possible promoters of hydride formation

In the opinion of some authors [35–37], the promoting effect of an element on hydride formation can be associated with its ability to form hydrides, for example, AsH$_3$, SbH$_3$, BiH$_3$, SnH$_4$, GeH$_4$. So we studied the activity of antimony and GeO$_2$, which were not used as promoters earlier. With Sb present in the solution, V_{NiH} fluctuates from 19 to 13%. A much lower hydride amount (~5%) was obtained in the solution with germanium oxide. Hence, antimony and germanium are acting as promoters, but their activity is much lower as compared with that of arsenic.

7.4 Studies of the state of arsenic on the surface of the charged nickel cathode
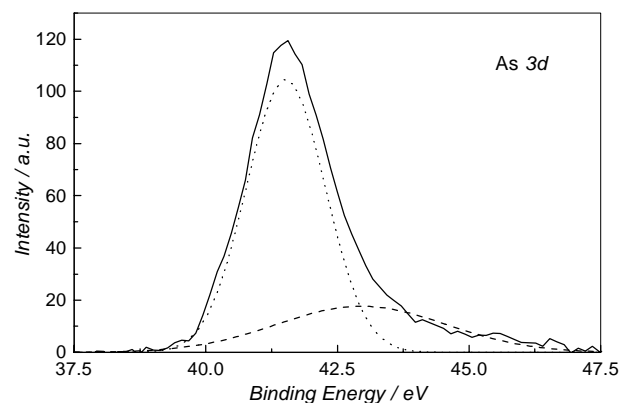
Fig. 16. As *3d* peak of XPS spectra from Ni electrode charged with hydrogen in 3 M KOH solution containing 0.2 g dm^{-3} of As$_2$O$_3$

As mentioned above, arsenic is detected on Ni electrode surface after the charging. An attempt was made to find out the state of arsenic by X-ray photoelectron spectroscopy. The spectrum of the electrode topmost surface showed that all arsenic was in a state of As$_2$O$_3$. After removing the very top of the surface by means of bombarding with Ar$^+$ ions, the quantity of As$_2$O$_3$ becomes significantly lower

and that of elemental arsenic higher. In the event of bombarding sample surface at a current density of 20 μA cm⁻² for 60 s, the whole amount of arsenic reaches 24–28 at. %, whereas the amount of oxygen falls to 0.8 at. %. A characteristic As *3d* peak of X-ray photoelectron spectrum is seen in Fig. 16. This peak (continuous curve) consists of two overlapping peaks. After their deconvolution it was obtained that the maximum of the more intensive peak (dot curve) corresponded to the binding energy value 41.50 eV characteristic of elemental arsenic, whereas the maximum of the less intensive peak (dashed curve) lay at a binding energy value of 42.95 eV. The binding energy typical of arsenic in the state of As_2O_3 is 44.4 eV [38], so the less portion of As must be in some another state, for example, in that of NiAs. Unfortunately, we failed to find in the literature the value of the binding energy of As characteristic of the latter compound. Our assumption that in this case NiAs can be formed is based on an analogy with NiS formation on Ni electrode charged in a solution containing thiourea. We have found that the maximum of the X-ray photoelectron spectrum peak S*2p* corresponds to the binding energy 162.3 eV, which is characteristic of sulphur in the state of NiS [38]. In the event our assumption on NiAs formation is right, the portion of arsenic in the state of NiAs on the charged Ni electrode, calculated from the areas of the separated As*3d* peaks, is about 7 at. %.

8. A possible mechanism of the promoter's accelerating action

The studies showed that the amount of hydride formed in alkaline solutions during the charging depends on the concentration of the promoter, current density and the duration of the charging. The maximum amount of β-NiH$_x$ phase is obtained when optimal values of these parameters are chosen. But the amount of nickel hydride does not depend on the nature or concentration of the alkali, at least in the case of KOH in a range from 0.5 to 6.0 M. Rather small amounts of hydride phase obtained by the authors of [14] can be related to non-optimal parameters of the charging process used by them: 1) a fairly high As_2O_3 concentration (1 instead of the necessary 0.2 g dm⁻³; 2) a rather high current of charging (300 instead of 100 mA cm⁻²); 3) a longer duration of the charging (120 instead of 30–40 min).

Antimony and germanium do act as promoters, but their activity is lower as compared with arsenic. So, in the sense of their activity the promoters can be arranged in the following row: S > As > Sb > Ge. When arranging these elements into rows, with regard to their activity in promoting the process of hydrogen penetration through a metal (Fe), some authors [35] obtained just the same row, whereas the others a bit different or even an opposite row [36].

Data of studies performed by X-ray photoelectron spectroscopy show that NiS and perhaps NiAs are formed during nickel charging. It is known [39] that the interaction of such metals as Ni, Fe, Co with such elements as S, As, Se, Te, Sb, Bi and sometimes with Ge and Sn results in the compounds of NiAs type. These B8$_1$ type compounds have a hexagonal lattice in which all octahedral cavities are filled up. With respect to atom packing density in a lattice, expressed by a ratio of the lattice parameters *c/a*, these compounds can be arranged into the following row:

Compound	NiS	NiSe	NiAs	Ni_3Sb_2	Ni_2Ge	Ni_3Sn_2
c/a	1.633	1.46	1.39	1.31	1.28	1.27

Since in this row the compounds containing S, As, Sb and Ge are arranged in the same order as in the row reflecting their activity when they act as promoters, we have formulated a hypothesis on the possibility of participation of NiAs type compounds in the process of hydride formation.

According to [40], the non-stoichiometric amorphous nickel sulphide Ni-S$_x$ shows a higher activity in hydrogen evolution reaction as compared to nickel. But after its heating for 4 h at 150 °C, when amorphous nickel sulphide is turned into crystallic one, Ni_2S_3, activity of the electrode becomes lower. When performing in acid and alkaline solutions electrochemical studies of hydrogen evolution on NiS, NiAs and NiSb, which possess a B8$_1$ structure, activity of these compounds in HER was found to be lower than that of pure nickel, particularly in acid solutions [41]. In this case the action of the promoters can be explained by formation of NiAs type compounds on the Ni cathode surface, which leads to a decrease in active surface and a corresponding increase in hydrogen current density and hydrogen chemical potential on the electrode surface. The chemical potential gradient of hydrogen, as a reason for hydride formation and its action in the role of a promoter, is also indicated by Conway and others [42].

CONCLUSIONS

The hydride formed in the course of cathodic charging of nickel [43] and its alloys [44] as well as its influence on the structure of metal and alloy at present are studied by XRD technique. Nevertheless, the a mechanism of hydride formation and its action in the role of a promoter remain not clear. There are to show that at a high pressure (> 3.5 Gpa) in hydrogen gas iron hydride is formed [45], but up to this day nobody has succeeded to determine whether FeH can be formed in the course of electrochemical processes. These questions can be answered by using the new possibilities of the XRD

method associated with XRD detectors of a new generation and a technique for studying thin layers. Magnetron-sputtered metal films can be used in XRD *in situ* studies of hydride formation, and thus the problem of film electrodeposited with high internal stresses could be solved.

References

1. B. Baranowski and M. Smialowski, *Bull. Acad. Polon. Ser. Scien. Chim.* **7** (1959) 663.
2. Z. Szklarska-Smialowska and M. Smialowski, *J. Electrochem. Soc.* **110** (1963) 444.
3. B. Baranowski and Z. Szklarska-Smialowska, *Electrochim. Acta* **9** (1964) 1497.
4. B. Baranowski and K. Bochenska, *Z. Phys. Chem.* **45** (1965) 140.
5. A. Janko, *Bull. Acad. Polon. Ser. Scien. Chim.* **8** (1960) 131.
6. A. Janko, *Bull. Acad. Polon. Ser. Scien. Chim.* **10** (1962) 617.
7. T. Boniszewski and G. C. Smith, *Phys. Chem. Solids* **21** (1961) 115.
8. A. Janko and J. Pielaszek, *Bull. Acad. Polon. Ser. Scien. Chim.* **15** (1967) 569.
9. J. E. Worsham, M. K. Wilkinson and C. G. Shull, *J. Phys. Chem. Solids* **3** (1957) 303.
10. St. Rashkov, M. Monev and I. Tomov, *Surf. Technology* **16** (1982) 203.
11. I. Tomov, M. Monev, M. Mikhailov and S. Rashkov, *J. Appl. Electrochem.* **22** (1992) 82.
12. J. Pielaszek, *Bull. Acad. Polon. Ser. Scien. Chim.* **20** (1972) 611.
13. I. Tomov and M. Monev, *J. Appl. Electrochem.* **22** (1992) 262.
14. M. Monev, M. E. Baumgartner, O. Loebich and Ch. J. Raub, *Metalloberflache*, **45** (1991) 77.
15. O. V. Urin, B. M. Platonov and J. M. Polukarov, *Elektrokhimiya*, **22** (1986) 1575.
16. D. M. Soares, O. Teschke and I. Torriani, *J. Electrochem. Soc.*, **139** (1992) 98.
17. B. Baranowski, *J. Electroanal. Chem.*, **472** (1999) 182.
18. B. Baranowski, *Roczniki chemii*, **38** (1964) 1019.
19. R. Juðkënas and V. Latvys, *Chemija (Vilnius)*, **3** (1992) 54.
20. R. Juðkënas, A. Selskis and V. Kadziauskienë, *Electrochim. Acta*, **43** (1998) 1903.
21. R. Juðkënas, R. Giraitis and V. Pakðtas, *Chemija (Vilnius)*, **13** (2002) 26.
22. R. Juðkënas, I. Valsiûnas, V. Jasulaitienë and V. Pakðtas, *Electrochim. Acta*, **47** (2002) 4239.
23. A. Vaðkelis, R. Juðkënas and J. Jaèiauskienë, *Electrochim. Acta*, **43** (1998) 1061.
24. S. Uno Falk, *J. Electrochem. Soc.*, **107** (1960) 661.
25. A. J. Salkind and P. F. Bruins, *J. Electrochem. Soc.*, **109** (1962) 356.
26. J. Burbank and C. P. Wales, *J. Electrochem. Soc.*, **111** (1964) 1002.
27. J. M. Polukarov and E. V. Semenova, *Elektrokhimiya*, **2** (1966) 79.
28. E. Langievka and A. Budniok, *Surf. Coat. Technology* **27** (1986) 57.
29. M. Fleischmann and A. Oliver, J. Robinson, *Electrochim. Acta*, **31** (1986) 899.
30. M. Fleischmann and B. W. Mao, *J. Electroanal and Interface Electrochem.* **229** (1987) 125.
31. M. Fleischmann and B. W. Mao, *J. Electroanal and Interface Electrochem.* **247** (1988) 297.
32. R. Juðkënas, V. Pakðtas, A. Sudavièius, V. Kapoèius and V. Karpavièienë, *Appl. Surf. Sci.* **229** (2004) 402.
33. Powder Diffraction File, (Edited by JCPDS) Swarthmore, Pennsylvania (1977).
34. J. W. Mellor, *A Comprehensive Treatise on Inorganic and Theoretical Chemistry*, Vol. 1, Longmans, London (1957).
35. P. K. Subramanyam, in Comprehensive Treatise of Electrochemistry (Ed. By J. O'M. Bockris, B. E. Conway, E. B. Yeager and R. E. White), Vol. 4, Plenum Press, New York, 1981, Ch. 8.
36. T. P. Radhakrishnan and L. L. Shreir, *Electrochim. Acta,* **11** (1966) 1007.
37. M. Monev, *Electrochim. Acta*, **46** (2001) 2373.
38. C. D. Wagner, W. M. Riggs, L. E. Davis, J. F. Moulder and G. E. Muilenberg, in: Handbook of X-Ray Photoelectron Spectroscopy, Perkin Elmer Corporation, Minnesota, 1978.
39. C. S. Barrett and T. B. Massalski, Structure of Metals, Pergamon Press, New York, 1980.
40. I. Paseka, *Electrochim. Acta*, **38** (1993) 2449.
41. A. K. M. Shamsul Huq and A. J. Rosenberg, *J. Electrochem. Soc.*, **111** (1964) 270.
42. B. E. Conway and G. Jerkiewicz, *J. Electroanal. Chem.*, **357** (1993) 47.
43. S. S. M. Tavares, S. Miraglia, D. Fruchart and D. S. dos Santos, *J. Alloys Comp.*, **347** (2002) 105.
44. S. S. M. Tavares, J. M. Pardal, T. Gurova, J. R. R. Bernardo and J. M. Neto, *J. Alloys Comp.*, **384** (2004) 152.
45. M. Tkacz, *J. Alloys Comp.*, **330–332** (2002) 25.

Remigijus Juðkënas

CHEMINIØ PROCESØ TYRIMAI RENTGENO DIFRAKCINIAIS *IN SITU* METODAIS.

METALØ HIDRIDØ, SUSIDARANÈIØ ELEKTROCHEMINIO VANDENILIO SKYRIMOSI METU, TYRIMAI

S a n t r a u k a

Apþvelgti nikelio hidrido susidarymo elektrocheminio vandenilio skyrimosi metu tyrimai. Ypaè daug dëmesio skirta Rentgeno spiduliø difrakcijos (RSD) metodo tiek *in situ*, tiek *ex situ* taikymui. Nagrinëjamas nikelio hidrido susidarymas rûgðtinëje ir ðarminëje terpëse su tokiais promotoriais, kaip tiourëja, As_2O_3, Sb ir GeO_2.